Journal of Sound and Vibration (1999) **224**(5), 809–841
Article No. jsvi.1999.2212, available online at http://www.idealibrary.com on IDEAL®

EFFECTS OF CENTRIFUGAL STIFFENING ON THE VIBRATION FREQUENCIES OF A CONSTRAINED FLEXIBLE ARM

E. H. K. FUNG AND D. T. W. YAU

Department of Mechanical Engineering, The Hong Kong Polytechnic University, Hung Hom, Kowloon, Hong Kong

(*Received* 24 *June* 1998, *and in final form* 15 *January* 1999)

A clamped-free rotating flexible robotic arm is modelled by the Euler–Bernoulli beam theory. The arm rotates horizontally about the clamped axis while the other end is constrained to move against a curve. The arm has an end mass attached at its tip. An axial compressive force, which is derived from the contact force between the tip of the arm and the constrained curve, is applied at the free end. When the flexible robotic arm rotates, a centrifugal force is produced on the arm by the centrifugal stiffening effect. Hamilton's principle is used to derive the equation of motion of the arm together with the associated boundary conditions. The non-homogeneous boundary condition is transformed into a homogeneous one by defining a new variable. The equation of motion and the boundary conditions are then expressed in non-dimensional form. The power series method is used to solve the equation of motion. A frequency equation is derived giving the relationship between the non-dimensional modal frequencies and the four non-dimensional parameters, i.e. the axially compressed force, the end mass, the angular velocity of the arm and the total moment of inertia about the hub. The numerical bisection method is used to solve for the natural frequencies under different values of axial force, end mass, angular velocity of the arm and the total moment of inertia about the hub. Results are prersented for the first three modes of vibration. These results are useful in the understanding of the dynamic behavior of the rotating constrained flexible beam with an end mass.

1. INTRODUCTION

Nowadays, industrial robots are mainly applied in two types of work. The first type of work is either dangerous or highly repetitive work. This type of work is usually performed in an unpleasant or dangerous environment. Examples include machining operation, welding, grinding and polishing, machine loading and unloading, forging and die-casting, spray painting, etc. The application of robots in this area can spare humans not only from many hazardous operations, but also from the boredom of much repetitive work. The second type of work is the kind that requires high precision and high speed of operation. This includes many assembly operations in the light industry and precision machining operations. The

0022-460X/99/300809 + 33 $30.00/0

application of robots in this area can increase the efficiency of the work and also improve the quality and the accuracy of the work produced.

In order to attain high speed of operation as required in the second type of work, the feasibility of using robot arms made of lightweight elastic links has been studied. The reduction in weight allows the robot arm to move faster and carry heavier loads with longer links. However, this reduction in weight has inevitably led to the problem of flexibility of the arm. When this robot arm is operating at high speed, the effects of flexibility of the arm cause the problem of oscillatory elastic motion. Also, the axial shortening of the arm due to centrifugal stiffening effects changes the system's natural frequencies. These in turn affect the precision of the robot motion. Hence, the axial shortening effect is an important area to be studied when investigating the vibration of a rotating flexible beam. In addition, there is a need to investigate the vibration of a rotating flexible beam under constrained motion. In many industrial applications of robot such as grinding and polishing, a constrained surface exists and the end of the last link of the robot experiences an axial compressive force resulting from the contact with the surface. Also, the end mass effect needs to be considered as the payload including the wrist or tool is usually present in many robotic applications. Moreover, in designing control algorithm for the robot arm, an accurate determination of the vibration frequencies of the flexible arm is necessary, as they are required by many model-based control methods. Hence, the objective of the present work is to investigate the effects of axial shortening on the vibration frequencies of a rotating constrained flexible robotic arm carrying an end mass.

Recently, the vibration of a rotating flexible beam has been studied by numerous researchers. Although exact frequency equations for the lateral vibrations of beams with different boundary conditions have been derived in many references [1–16], not many of them have taken into account the axial shortening effect in their studies. Among those that have not considered the axial shortening effect [1–7], some even did not consider the end mass effect. Liu and Ertekin [5] presented the results of a free–free beam under both tensile and compressive load and the fundamental frequency is found for the tensile case. However, the above analyses were performed on the axial compressive or tensile beams without the end mass. There is a need to consider, in addition to the constrained force effect, the end mass effect in the derivation of the frequency characteristic equation as the payload is usually present in many robotic applications as mentioned earlier in this paper. Moreover, White and Heppler [6, 7] studied the vibration of a rotating Timoshenko beam with an attached end mass using two different rotating frames of reference: pseudo-pinned and pseudo-clamped, but the axial shortening effect due to the centrifugal stiffening is not considered in his paper.

The axial shortening due to the centrifugal stiffening effects of the rotating beam was also a topic considered by many researchers [8–15]. Among them, some analyzed the end mass in their models [11–15] while others did not study its effects [8–10]. Yigit *et al.* [8, 9] formulated a model of a rotating Euler–Bernoulli beam that includes the axial shortening effect. Du *et al.* [12] employed the Timoshenko beam model to formulate the equations of motion of a rotating beam that has a finite hub and has a mass attached at the free end of the beam. This model

includes the effect of centrifugal stiffening due to constant angular rotation and the resulting equations of motion are solved by the power series method. Also, Fallahi *et al.* [14] utilized a Timoshenko beam model to formulate a rotating beam–mass system with centrifugal stiffening effect. In this paper, the effects of speed and tip mass on the cross-coupling between the elastic and rigid-body motions represented by Coriolis, normal and tangential accelerations are investigated. However, for all the above studies [8–15], the robotic arm under investigation is not subjected to any axial compressive force. Fung and Shi [16] in a recent paper has formulated a model of a rotating Euler–Bernoulli beam that carries an end mass and is subjected to an axial compressive force. In this paper, an exact frequency equation is derived giving the relationship between the vibration frquencies and the parameters such as the axial compressive force and the end mass. However, the effect of axial shortening was not considered and hence the parameter of the beam angular velocity was not included in the frequency equation.

The present study aims to determine the natural vibration frequencies of a rotating constrained flexible arm carrying an end mass taking into consideration the axial shortening effect. In this paper, the robotic arm is modelled by a clamped–free Euler–Bernoulli beam ignoring the shear deformation and rotary inertia effects. The arm rotates horizontally about the clamped axis while the free end is constrained to move against a curve. The arm also has an end mass attached at its tip. An axial compressive force derived from the contact force between the tip of the arm and the constrained curve is applied at the free end. When the flexible robotic arm rotates, an axial shortening force is produced on the arm by the centrifugal stiffening effect. Hamilton's principle is used to derive the governing equation of motion of the beam along with the boundary conditions. The non-homogeneous boundary condition is transformed into a homogeneous one by defining a new variable. The equation of motion and the boundary condition are then expressed in non-dimensional form. The power series method is used to solve the equation of motion. A frequency equation is derived giving the relationship between the non-dimensional modal frequencies and the four non-dimensional parameters, i.e., the axially compressed force, the end mass, the angular velocity of the arm and the total moment of inertia about the hub. Numerical bisection method is used to solve for the natural frequencies under different values of axial force, end mass, angular velocity of the arm and total moment of inertia about the hub by means of FORTRAN programming. Results are presented for the first three modes of vibration. These results are useful in understanding the dynamic behavior of the rotating constrained flexible beam carrying an end mass.

2. THEORY

The clamped–free flexible robotic arm to be studied is shown in Figure 1. It is modelled by the Euler–Bernoulli beam theory in which rotary inertia and shear deformation effects are ignored. The arm is of length L and the mass per unit length is ρ. It rotates at an angular velocity of $\dot{\theta}$ about the clamped axis and has a mass m attached at its free end. The end is also constrained to move against a curve

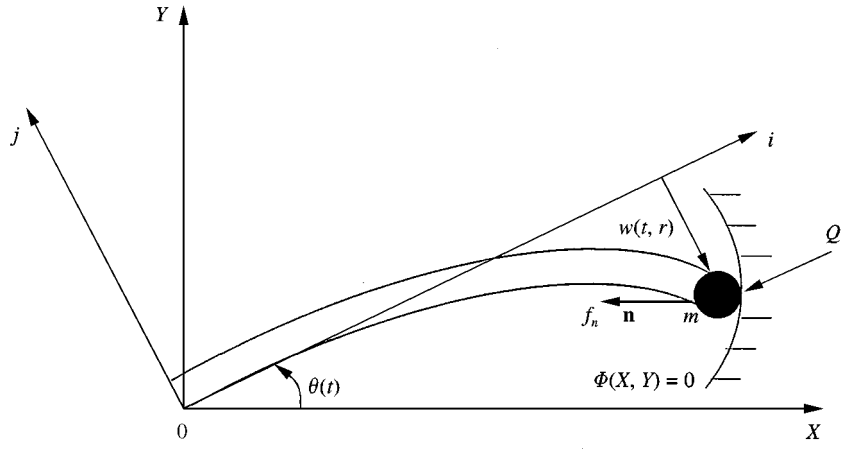

Figure 1. A rotating constrained flexible robotic arm carrying an end mass.

$\Phi(X, Y) = 0$. An axial compressive force Q which is derived from the contact force between the tip of the arm and the constrained curve is applied at the free end. When this flexible robotic arm rotates, the centrifugal stiffening effect will produce a centrifugal force $P(r, t)$ on the arm. The work done by this centrifugal force will produce an axial shortening effect on the arm.

The transverse displacement of a spatial point on the beam at a distance $r(0 < r < L)$ from the origin is denoted by $w(t, r)$ while the transverse displacement at the tip end is denoted by $w_E(t)$ where

$$w_E(t) = w(t, L).$$

Let (X_p, Y_p) denote the co-ordinates of the end point of the beam in the inertial Cartesian axes OXY. Then

$$X_p = L\cos\theta + w_E \sin\theta, \quad Y_p = L\sin\theta - w_E\cos\theta$$

The position vector $\mathbf{P}$ of the end mass m and the position vector $\mathbf{r}$ of a spatial point at a distance r from the origin of the flexible link are

$$\mathbf{P} = L\mathbf{i} - w_E\mathbf{j}, \qquad \dot{\mathbf{P}} = w_E\dot{\theta}\mathbf{i} + L\dot{\theta}\mathbf{j} - \dot{w}_E\mathbf{j},$$
$$\mathbf{r} = r\mathbf{i} - w(t, r)\mathbf{j}, \quad \dot{\mathbf{r}} = w(t, r)\dot{\theta}\mathbf{i} + r\dot{\theta}\mathbf{j} - \dot{w}(t, r)\mathbf{j} \tag{1}$$

Let EI be the flexural rigidity of the beam, J the moment of inertia of the hub and $P(r, t)$ the centrifugal force arising from the centrifugal stiffening effect.

The total kinetic energy T of the system is

$$T = \frac{1}{2}\int_0^L \rho\dot{\mathbf{r}}^{\mathrm{T}}\dot{\mathbf{r}}\,\mathrm{d}r + \frac{1}{2}m\dot{\mathbf{P}}^{\mathrm{T}}\dot{\mathbf{P}} + \frac{1}{2}J\dot{\theta}^2$$
$$= \frac{1}{2}\int_0^L \rho(w^2\dot{\theta}^2 + r^2\dot{\theta}^2 + \dot{w}^2 - 2r\dot{\theta}\dot{w})\,\mathrm{d}r + \frac{1}{2}m(w_E^2\dot{\theta}^2 + L^2\dot{\theta}^2 + \dot{w}_E^2 - 2L\dot{\theta}\dot{w}_E) \tag{2}$$
$$+ \frac{1}{2}J\dot{\theta}^2$$

and the total potential energy V of the system is

$$V = \frac{1}{2}\int_0^L EI(w'')^2\,\mathrm{d}r - \frac{1}{2}\int_0^L Q(w')^2\,\mathrm{d}r + \frac{1}{2}\int_0^L P(r,t)(w')^2\,\mathrm{d}r, \tag{3}$$

where a dot denotes the time derivative and a prime denotes the derivative with respect to the spatial variable r and

$$P(r,t) = mL\dot{\theta}^2 + \int_r^L \rho r\dot{\theta}^2\,\mathrm{d}r$$

$$= mL\dot{\theta}^2 + \frac{1}{2}\rho\dot{\theta}^2(L^2 - r^2). \tag{4}$$

The virtual work done by the applied torque δW is given by

$$\delta W = \tau\delta\theta, \tag{5}$$

where τ is the applied hub torque.

By applying Hamilton's principle,

$$\int_{t_1}^{t_2} (\delta T - \delta V + \delta W + \lambda\delta\Phi)\,\mathrm{d}t \equiv 0, \tag{6}$$

where λ is a Lagrange multiplier.

Assuming that E, I. ρ, L are constants and substituting equations (1)–(5) into equation (6), the equation of vibration of the flexible beam can be obtained. The equation of vibration of the flexible beam is

$$\rho(r\ddot{\theta} - \ddot{w} + \dot{\theta}^2 w) - EIw'''' - Qw'' + [\tfrac{1}{2}\rho\dot{\theta}^2(L^2 - r^2) + mL\dot{\theta}^2]w'' - \rho\dot{\theta}^2 rw' = 0. \tag{7}$$

The four boundary conditions at the clamped end and the constrained end are

$$w(t,0) = 0, \qquad w'(t,0) = 0, \qquad w''_E = w''(t,L) = 0, \tag{8a–c}$$

$$EI\left(\frac{m}{\rho}w''''_E + w'''_E\right) + Qw'_E = -\lambda\frac{\partial\Phi}{\partial w_E}. \tag{8d}$$

Since the boundary condition given by equation (8d) is non-homogeneous, it is difficult to treat it directly. This non-homogeneous boundary condition is therefore transformed into a homogeneous one [16] by defining a new variable $v(t,r)$. Let

$$v(t,r) = w(t,r) + g(t)f(r) \tag{9}$$

where

$$g(t) = \lambda\frac{\partial\Phi}{\partial w_E}$$

and

$$f(r) = \frac{1}{EI}\left(\frac{L}{2}r^2 - \frac{5}{6}r^3 + \frac{1}{2L}r^4 - \frac{1}{10L^2}r^5\right).$$

$g(t)$ and $f(r)$ are selected to satisfy the boundary conditions in equations (8a)–(8d). Substituting equation (9) into equation (7) and retaining the terms that are needed for the determination of the natural frequencies gives the following equation of motion:

$$EIv'''' + (Q - \tfrac{1}{2}\rho\dot{\theta}^2L^2 - mL\dot{\theta}^2 + \tfrac{1}{2}\rho\dot{\theta}^2r^2)v'' + \rho\dot{\theta}^2rv' + \rho\ddot{v} - \rho\dot{\theta}^2v - \rho r\ddot{\theta} = 0. \tag{10}$$

Substituting equation (9) into equations (8a)–(8d), the non-homogeneous boundary condition is transformed into a homogeneous one in v:

$$v(t, 0) = 0, \quad v'(t, 0) = 0, \quad v''_E = v''(t, L) = 0, \tag{11a–c}$$

$$EI\left(\frac{m}{\rho}v''''_E + v'''_E\right) + Qv'_E = 0. \tag{11d}$$

The method of assumed modes is applied, so the variable v is expressed as

$$v(t, r) = \sum_{i=1}^{\infty} Y_i(r)q_i(t). \tag{12}$$

Substituting equation (12) into equation (10), we obtain

$$\sum_{i=1}^{\infty} \{EIY''''_i(r)q_i(t) + (Q - \tfrac{1}{2}\rho\dot{\theta}^2L^2 - mL\dot{\theta}^2 + \tfrac{1}{2}\rho\dot{\theta}^2r^2)Y''_i(r)q_i(t) + \rho\dot{\theta}^2rY'_i(r)q_i(t) + \rho Y_i(r)\ddot{q}_i(t) - \rho\dot{\theta}^2Y_i(r)q_i(t)\} = \rho r\ddot{\theta}. \tag{13}$$

Torque balance about the hub gives

$$J_t\ddot{\theta} = \tau - \tau_1, \tag{14}$$

where J_t is the total moment of inertia about the hub and

$$\tau_1 = \int_0^L \rho r\ddot{w}\,\mathrm{d}r + mL\ddot{w}_E + Qw_E. \tag{15}$$

Combining equations (14) and (15), setting $\tau = 0$ for free vibration of the beam and ignoring the terms that are not required for the determination of the natural frequencies, we obtain

$$J_t\ddot{\theta} = -\int_0^L \rho r\ddot{v}\,\mathrm{d}r - mL\ddot{v}_E - Qv_E. \tag{16}$$

Using equations (12) and (16), the following equation is obtained:

$$J_t\ddot{\theta} = -\int_0^L \rho r \sum_{i=1}^{\infty} Y_i(r)\ddot{q}_i(t)\,\mathrm{d}r - mL\sum_{i=1}^{\infty} Y_i(L)\ddot{q}_i(t) - Q\sum_{i=1}^{\infty} Y_i(L)q_i(t). \quad (17)$$

Combining equations (13) and (17) and considering the ith mode, we have

$$EIY_i''''q_i + (Q - \tfrac{1}{2}\rho\dot{\theta}^2L^2 - mL\dot{\theta}^2 + \tfrac{1}{2}\rho\dot{\theta}^2r^2)Y_i''q_i + \rho\dot{\theta}^2rY_i'q_i + \rho Y_i\ddot{q}_i$$
$$- \rho\dot{\theta}^2Y_iq_i + \frac{\rho r}{J_i}\left(\int_0^L \rho rY_i\ddot{q}_i\,\mathrm{d}r + mLY_i(L)\ddot{q}_i + QY_i(L)q_i\right) = 0.$$

Therefore,

$$EIY_i'''' + (Q - \tfrac{1}{2}\rho\dot{\theta}^2L^2 - mL\dot{\theta}^2 + \tfrac{1}{2}\rho\dot{\theta}^2r^2)Y_i'' + \rho\dot{\theta}^2rY_i' - \rho\dot{\theta}^2Y_i$$
$$+ \frac{\rho r}{J_t}QY_i(L) = -\left[\rho Y_i + \frac{\rho r}{J_t}\left\{\int_0^L \rho rY_i\,\mathrm{d}r + mLY_i(L)\right\}\right]\frac{\ddot{q}_i}{q_i}. \quad (18)$$

Assuming harmonic vibration, the equation for the generalized co-ordinate is

$$\ddot{q}_i(t) = -\omega_i^2q_i(t), \quad (19)$$

where ω_i is the vibration frequency of the rotating beam.

Using equations (18) and (19), the following equation for the mode shape function can be obtained:

$$EIY_i'''' + (Q - \tfrac{1}{2}\rho\dot{\theta}^2L^2 - mL\dot{\theta}^2 + \tfrac{1}{2}\rho\dot{\theta}^2r^2)Y_i'' + \rho\dot{\theta}^2rY_i' - \rho\dot{\theta}^2Y_i$$
$$+ \frac{\rho r}{J_t}QY_i(L) - \rho Y_i\omega_i^2 - \frac{\rho r\omega_i^2}{J_t}\left\{\int_0^L \rho rY_i\,\mathrm{d}r + mLY_i(L)\right\} = 0.$$

Defining

$$\mu_i = -\int_0^L \rho r\omega_i^2Y_i(r)\mathrm{d}r - mL\omega_i^2Y_i(L) + QY_i(L), \quad (20a)$$

we obtain

$$EIY_i'''' + (Q - \tfrac{1}{2}\rho\dot{\theta}^2L^2 - mL\dot{\theta}^2 + \tfrac{1}{2}\rho\dot{\theta}^2r^2)Y_i''$$
$$+ \rho\dot{\theta}^2rY_i' - \rho\omega_i^2Y_i - \rho\dot{\theta}^2Y_i = -\rho r\mu_i/J_t. \quad (20b)$$

Substituting equation (12) into equations (11a)–(11d) yields the following boundary conditions in Y_i:

$$Y_i(0) = 0, \quad Y_i'(0) = 0, \quad Y_i''(L) = 0, \quad (21a, c)$$

$$EIY_i'''(L) + QY_i'(L) = 0. \quad (21d)$$

Introducing the non-dimensional parameters

$$\xi = \frac{r}{L}, \quad N = \frac{m}{\rho L}, \quad U = \frac{QL^2}{EI}$$

$$J_0 = \frac{J_t}{\rho L^3}, \quad \eta = \sqrt{\frac{\rho}{EI}}\,\dot{\theta} L^2, \quad \Omega_i = \sqrt{\frac{\rho}{EI}}\,\omega_i L^2,$$

the following equation for the mode shape function can be obtained:

$$Y_i'''' + (U - \tfrac{1}{2}\eta^2 - N\eta^2 + \tfrac{1}{2}\eta^2\xi^2) Y_i'' + \eta^2 \xi Y_i' - \Omega_i^2 Y_i - \eta^2 Y_i = -(\mu_0/J_0)\xi, \quad (22)$$

where a prime ( )′ denotes the derivative with respect to the non-dimensional co-ordinate ξ and

$$\mu_0 = -\int_0^1 \xi \Omega_i^2 Y_i(\xi)\,\mathrm{d}\xi - N\Omega_i^2 Y_i(1) + U Y_i(1). \quad (23)$$

Defining

$$C_1 = U - \tfrac{1}{2}\eta^2 - N\eta^2, \qquad C_2 = \tfrac{1}{2}\eta^2,$$

$$C_3 = -\Omega_i^2 - \eta^2, \qquad C_4 = -\frac{\mu_0}{J_0},$$

the equation of motion (22) of the flexible beam becomes

$$Y_i'''' + (C_1 + C_2\xi^2) Y_i'' + 2C_2\xi Y_i' + C_3 Y_i = C_4\xi, \quad (24)$$

where Y_i is now a function of ξ instead of r.

Substituting the non-dimensional parameters into equations (21a)–(21d), the four boundary conditions become

$$Y_i(0) = 0, \quad Y_i'(0) = 0, \quad Y_i''(1) = 0, \quad (25a\text{–}c)$$

$$N Y_i''''(1) + Y_i'''(1) + U Y_i'(1) = 0. \quad (25d)$$

Equation (24) is a non-homogeneous differential equation with variable coefficients. The total solution of this equation can be expressed in terms of a homogeneous solution and a particular solution in the form

$$Y_i(\xi) = Y_{ic}(\xi) + F\xi, \quad (26)$$

where $Y_i(\xi)$ is the total solution, $Y_{ic}(\xi)$ is the homogeneous solution and $F\xi$ is the particular solution. Substituting equation (26) and their derivatives into equation (24), the equation for the homogeneous solution $Y_{ic}(\xi)$ and the constant F are found to be

$$Y_{\mathrm{ic}}'''' + (C_1 + C_2\xi^2) Y_{\mathrm{ic}}'' + 2C_2\xi Y_{ic}' + C_3 Y_{ic} = 0, \quad (27)$$

$$F = \frac{\mu_0}{J_0\Omega_i^2} = \frac{-1}{J_0\Omega_i^2}\left[\int_0^1 \xi\Omega_i^2 Y_i(\xi)\,\mathrm{d}\xi + N\Omega_i^2 Y_i(1) - U Y_i(1)\right]. \quad (28)$$

The homogeneous equation (27) is solved by the power series method as described in the next section.

3. POWER SERIES SOLUTION OF THE MODE SHAPE EQUATION

Equation (27) is a variable coefficient differential equation that cannot be solved analytically by using ordinary trigonometric or hyperbolic functions. Hence, the power series method is used in this case by expressing the homogeneous solution $Y_{ic}(\xi)$ as a power series in the independent variable ξ.

Let

$$u(\xi) = \sum_{k=0}^{\infty} a_k \xi^k = a_0 + a_1\xi + a_2\xi^2 + a_3\xi^3 + \cdots,$$

$$u'(\xi) = \sum_{k=1}^{\infty} k a_k \xi^{k-1} = \sum_{k=0}^{\infty} (k+1) a_{k+1} \xi^k,$$

$$u''(\xi) = \sum_{k=2}^{\infty} k(k-1) a_k \xi^{k-2} = \sum_{k=1}^{\infty} (k+1)k a_{k+1} \xi^{k-1} = \sum_{k=0}^{\infty} (k+2)(k+1) a_{k+2}\, \xi^k,$$

$$u'''(\xi) = \sum_{k=3}^{\infty} k(k-1)(k-2) a_k \xi^{k-3} = \sum_{k=2}^{\infty} (k+1)\mathrm{k}(k-1) a_{k+1} \xi^{k-2}$$

$$= \sum_{k=1}^{\infty} (k+2)(k+1)k a_{k+2}\, \xi^{k-1} = \sum_{k=0}^{\infty} (k+3)(k+2)(k+1) a_{k+3}\, \xi^k$$

$$u''''(\xi) = \sum_{k=4}^{\infty} k(k-1)(k-2)(k-3) a_k \xi^{k-4} = \sum_{k=3}^{\infty} (k+1)k(k-1)(k-2) a_{k+1} \xi^{k-3}$$

$$= \sum_{k=2}^{\infty} (k+2)(k+1)k(k-1) a_{k+2}\, \xi^{k-2} = \sum_{k=1}^{\infty} (k+3)(k+2)(k+1)k a_{k+3}\, \xi^{k-1}$$

$$= \sum_{k=0}^{\infty} (k+4)(k+3)(k+2)(k+1) a_{k+4} \xi^k. \tag{29}$$

Substituting equation (29) into equation (27) gives

$$(k+4)(k+3)(k+2)(k+1) a_{k+4} \xi^k + C_1(k+2)(k+1) a_{k+2} \xi^k + C_2 k(k-1) a_k \xi^k$$
$$+ 2C_2 k a_k \xi^k + C_3 a_k \xi^k = 0.$$

Equating coefficients of like power of ξ yields the recurrence formula

$$a_{k+4} = -\frac{C_1 a_{k+2}}{(k+4)(k+3)}$$
$$-\left[\frac{kC_2}{(k+4)(k+3)(k+2)} + \frac{C_3}{(k+4)(k+3)(\mathrm{k}+2)(k+1)}\right] a_k, \quad k \geqslant 0. \tag{30}$$

There are four arbitrary constants a_0, a_1, a_2, a_3 in equation (29). Four linearly independent solutions u_0, u_1, u_2, u_3 can be obtained by selecting these four arbitrary constants as follows:

$$\begin{aligned}
&\text{for } u_0, \quad a_0 = 1 \quad \text{and} \quad a_1 = a_2 = a_3 = 0,\\
&\text{for } u_1, \quad a_0 = 0 \quad \text{and} \quad a_1 = 1,\ a_2 = a_3 = 0,\\
&\text{for } u_2, \quad a_0 = a_1 = 0 \quad \text{and} \quad a_2 = 1, \quad a_3 = 0,\\
&\text{for } u_3, \quad a_0 = a_1 = a_2 = 0 \quad \text{and } a_3 = 1.
\end{aligned} \tag{31}$$

These four linearly independent functions can be written explicitly as

$$\begin{aligned}
u_0(\xi) &= 1 - \frac{C_3}{24}\xi^4 + \frac{C_1 C_3}{720}\xi^6 + \cdots,\\
u_1(\xi) &= \xi - \frac{2C_2 + C_3}{120}\xi^5 + \frac{(2C_2 + C_3)C_1}{5040}\xi^7 + \cdots,\\
u_2(\xi) &= \xi^2 - \frac{C_1}{12}\xi^4 + \frac{C_1^2 - 6C_2 - C_3}{360}\xi^6 + \cdots,\\
u_3(\xi) &= \xi^3 - \frac{C_1}{20}\xi^5 + \frac{C_1^2 - 12C_2 - C_3}{840}\xi^7 + \cdots.
\end{aligned} \tag{32}$$

The linear combination of these four linearly independent functions is the homogeneous solution of equation (27), and can be written as

$$Y_{ic}(\xi) = \lambda_0 u_0(\xi) + \lambda_1 u_1(\xi) + \lambda_2 u_2(\xi) + \lambda_3 u_3(\xi). \tag{33}$$

The total solution of equation (24) is

$$Y_i(\xi) = \lambda_0 u_0(\xi) + \lambda_1 u_1(\xi) + \lambda_2 u_2(\xi) + \lambda_3 u_3(\xi) + F\xi, \tag{34}$$

where $\lambda_0, \lambda_1, \lambda_2, \lambda_3$ are constants to be determined by the four boundary conditions given by equations (25a)–(25d). From equations (25a), (32) and (34)

$$Y_i(0) = \lambda_0 = 0. \tag{35}$$

From equations (25b), (32) and (34)

$$Y_i'(0) = \lambda_1 + F = 0. \tag{36}$$

Substituting equation (35) into equation (34), we obtain

$$Y_i(\xi) = \lambda_1 u_1(\xi) + \lambda_2 u_2(\xi) + \lambda_3 u_3(\xi) + F\xi. \tag{37}$$

From equations (25c) and (37),

$$Y_i''(1) = \lambda_1 u_1''(1) + \lambda_2 u_2''(1) + \lambda_3 u_3''(1) = 0. \tag{38}$$

From equation (37), we have

$$Y_i'(1) = \lambda_1 u_1'(1) + \lambda_2 u_2'(1) + \lambda_3 u_3'(1) + F,$$
$$Y_i'''(1) = \lambda_1 u_1'''(1) + \lambda_2 u_2'''(1) + \lambda_3 u_3'''(1),$$
$$Y_i''''(1) = \lambda_1 u_1''''(1) + \lambda_2 u_2''''(1) + \lambda_3 u_3''''(1). \tag{39}$$

Substituting equation (39) into equation (25d) gives

$$[Nu_1''''(1) + u_1'''(1) + U(u_1'(1) - 1)]\lambda_1 + [Nu_2''''(1) + u_2'''(1) + Uu_2'(1)]\lambda_2 + [Nu_3''''(1) + u_3'''(1) + Uu_3'(1)]\lambda_3 = 0. \tag{40}$$

Equations (36), (38) and (40) can be written in the following matrix form:

$$\begin{bmatrix} 1 & 0 & 0 \\ u_1''(1) & u_2''(1) & u_3''(1) \\ Nu_1''''(1) + u_1'''(1) + U(u_1'(1) - 1) & Nu_2''''(1) + u_2'''(1) + Uu_2'(1) & Nu_3''''(1) + u_3'''(1) + Uu_3'(1) \end{bmatrix} \times \begin{Bmatrix} \lambda_1 \\ \lambda_2 \\ \lambda_3 \end{Bmatrix} = \begin{bmatrix} -F \\ 0 \\ 0 \end{bmatrix} \tag{41}$$

which yields

$$\lambda_1 = -F, \tag{42}$$

$$\lambda_2 = \frac{[Nu_3''''(1) + u_3'''(1) + Uu_3'(1)]u_1''(1) - [Nu_1''''(1) + u_1'''(1) + U(u_1'(1) - 1)]u_3''(1)}{[Nu_3''''(1) + u_3'''(1) + Uu_3'(1)]u_2''(1) - [Nu_2''''(1) + u_2'''(1) + Uu_2'(1)]u_3''(1)} F, \tag{43}$$

$$\lambda_3 = \frac{[Nu_1''''(1) + u_1'''(1) + U(u_1'(1) - 1)]u_2''(1) - [Nu_2''''(1) + u_2'''(1) + Uu_2'(1)]u_1''(1)}{[Nu_3''''(1) + u_3'''(1) + Uu_3'(1)]u_2''(1) - [Nu_2''''(1) + u_2'''(1) + Uu_2'(1)]u_3''(1)} F. \tag{44}$$

Substituting equations (37) and (42)–(44) into equation (28), one obtains the following frequency equation relating the non-dimensional modal frequencies Ω_i to the axial force U, the end mass N, the beam angular velocity η and the total moment of inertia about the hub J_0:

$$D_1\Omega_i^2 + D_2 N\Omega_i^2 - D_2 U - J_0\Omega_i^2 = 0, \tag{45}$$

where

$$D_1 = \frac{[Nu_1''''(1) + u_1'''(1) + U(u_1'(1) - 1)]u_3''(1) - [Nu_3''''(1) + u_3'''(1) + Uu_3'(1)]u_1''(1)}{[Nu_3''''(1) + u_3'''(1) + Uu_3'(1)]u_2''(1) - [Nu_2''''(1) + u_2'''(1) + Uu_2'(1)]u_3''(1)} \int_0^1 \xi u_2(\xi)\,\mathrm{d}\xi + \frac{[Nu_2''''(1) + u_2'''(1) + Uu_2'(1)]u_1''(1) - [Nu_1''''(1) + u_1'''(1) + U(u_1'(1) - 1)]u_2''(1)}{[Nu_3''''(1) + u_3'''(1) + Uu_3'(1)]u_2''(1) - [Nu_2''''(1) + u_2'''(1) + Uu_2'(1)]u_3''(1)} \times \int_0^1 \xi u_3(\xi)\,\mathrm{d}\xi + \int_0^1 \xi u_1(\xi)\,\mathrm{d}\xi - \frac{1}{3} \tag{46}$$

$$D_2 = \frac{[Nu_1''''(1) + u_1'''(1) + U(u_1'(1) - 1)]u_3''(1) - [Nu_3''''(1) + u_3'''(1) + Uu_3'(1)]u_1''(1)}{[Nu_3''''(1) + u_3'''(1) + Uu_3'(1)]u_2''(1) - [Nu_2''''(1) + u_2'''(1) + Uu_2'(1)]u_3''(1)} u_2(1)$$

$$+ \frac{[Nu_2''''(1) + u_2'''(1) + Uu_2'(1)]u_1''(1) - [Nu_1''''(1) + u_1'''(1) + U(u_1'(1) - 1)]u_2''(1)}{[Nu_3''''(1) + u_3'''(1) + Uu_3'(1)]u_2''(1) - [Nu_2''''(1) + u_2'''(1) + Uu_2'(1)]u_3''(1)} u_3(1)$$

$$+ u_1(1) - 1. \tag{47}$$

Using equations (29) and (31), the spatial derivatives and integral of u_1, u_2 and u_3 can be obtained. For u_1, $a_0 = 0$ and $a_1 = 1$, $a_2 = a_3 = 0$

$$\int_0^1 \xi u_1(\xi)\,\mathrm{d}\xi = \frac{1}{3} + \sum_{k=0}^{\infty} \frac{a_{k+4}}{k+6}, \tag{48}$$

$$u_1(1) = 1 + \sum_{k=0}^{\infty} a_{k+4}, \tag{49}$$

$$u_1'(1) = 1 + \sum_{k=0}^{\infty} (k+4)a_{k+4}, \tag{50}$$

$$u_1''(1) = \sum_{k=0}^{\infty} (k+4)(k+3)a_{k+4}, \tag{51}$$

$$u_1'''(1) = \sum_{k=0}^{\infty} (k+4)(k+3)(k+2)a_{k+4}, \tag{52}$$

$$u_1''''(1) = \sum_{k=0}^{\infty} (k+4)(k+3)(k+2)(k+1)a_{k+4}. \tag{53}$$

For u_2, $a_0 = a_1 = 0$ and $a_2 = 1$, $a_3 = 0$,

$$\int_0^1 \xi u_2(\xi)\,\mathrm{d}\xi = \frac{1}{4} + \sum_{k=0}^{\infty} \frac{a_{k+4}}{k+6}, \tag{54}$$

$$u_2(1) = 1 + \sum_{k=0}^{\infty} a_{k+4}, \tag{55}$$

$$u_2'(1) = 2 + \sum_{k=0}^{\infty} (k+4)a_{k+4}, \tag{56}$$

$$u_2''(1) = 2 + \sum_{k=0}^{\infty} (k+4)(k+3)a_{k+4}, \tag{57}$$

$$u_2'''(1) = \sum_{k=0}^{\infty} (k+4)(k+3)(k+2)a_{k+4}, \tag{58}$$

$$u_2''''(1) = \sum_{k=0}^{\infty} (k+4)(k+3)(k+2)(k+1)a_{k+4}. \tag{59}$$

TABLE 1

Non-dimensional first modal frequencies Ω_1 under different end masses N, axial forces U and beam angular velocities η for $J_0 = 3$

		First mode Ω_1						
N	U	$\eta = 0$	$\eta = 0{\cdot}5$	$\eta = 1{\cdot}0$	$\eta = 1{\cdot}5$	$\eta = 2{\cdot}0$	$\eta = 2{\cdot}5$	$\eta = 3{\cdot}0$
0	0	3·340	3·347	3·366	3·398	3·441	3·494	3·556
	0·617	2·957	2·965	2·988	3·026	3·077	3·140	3·213
	1·234	2·496	2·506	2·536	2·584	2·648	2·726	2·815
	1·851	1·902	1·916	1·957	2·024	2·111	2·215	2·332
	2·465	0·945	0·975	1·061	1·189	1·343	1·514	1·693
1	0	1·298	1·311	1·348	1·404	1·473	1·550	1·631
	0·617	1·191	1·206	1·248	1·310	1·387	1·470	1·557
	1·234	1·071	1·088	1·137	1·208	1·293	1·385	1·479
	1·851	0·934	0·954	1·011	1·094	1·191	1·293	1·396
	2·465	0·770	0·796	0·867	0·966	1·079	1·194	1·308
2	0	0·870	0·886	0·929	0·990	1·060	1·133	1·206
	0·617	0·830	0·847	0·893	0·958	1·032	1·109	1·184
	1·234	0·786	0·805	0·856	0·926	1·004	1·084	1·162
	1·851	0·739	0·760	0·815	0·891	0·974	1·058	1·140
	2·465	0·688	0·711	0·773	0·855	0·944	1·032	1·117
3	0	0·664	0·681	0·726	0·787	0·854	0·921	0·985
	0·617	0·656	0·674	0·721	0·784	0·852	0·920	0·986
	1·234	0·648	0·667	0·716	0·781	0·851	0·920	0·987
	1·851	0·639	0·659	0·711	0·778	0·850	0·920	0·987
	2·465	0·629	0·650	0·705	0·775	0·848	0·920	0·988
4	0	0·539	0·557	0·603	0·662	0·725	0·786	0·844
	0·617	0·551	0·570	0·616	0·676	0·738	0·798	0·857
	1·234	0·563	0·581	0·628	0·688	0·751	0·811	0·869
	1·851	0·574	0·593	0·640	0·701	0·763	0·823	0·881
	2·465	0·584	0·603	0·652	0·713	0·775	0·836	0·893

For u_3, $a_0 = a_1 = a_2 = 0$, and $a_3 = 1$

$$\int_0^1 \xi u_3(\xi)\,\mathrm{d}\xi = \frac{1}{5} + \sum_{k=0}^{\infty} \frac{a_{k+4}}{k+6}, \tag{60}$$

$$u_3(1) = 1 + \sum_{k=0}^{\infty} a_{k+4}, \tag{61}$$

$$u_3'(1) = 3 + \sum_{k=0}^{\infty} (k+4)a_{k+4}, \tag{62}$$

$$u_3''(1) = 6 + \sum_{k=0}^{\infty} (k+4)(k+3)a_{k+4}, \tag{63}$$

$$u_3'''(1) = 6 + \sum_{k=0}^{\infty} (k+4)(k+3)(k+2)a_{k+4}, \tag{64}$$

$$u_3''''(1) = \sum_{k=0}^{\infty} (k+4)(k+3)(k+2)(k+1)a_{k+4}. \tag{65}$$

TABLE 2

Non-dimensional second modal frequencies Ω_2 under different end masses N, axial forces U and beam angular velocities η for $J_0 = 3$

		Second mode Ω_2						
N	U	$\eta = 0$	$\eta = 0{\cdot}5$	$\eta = 1{\cdot}0$	$\eta = 1{\cdot}5$	$\eta = 2{\cdot}0$	$\eta = 2{\cdot}5$	$\eta = 3{\cdot}0$
0	0	22·007	22·038	22·132	22·286	22·500	22·773	23·102
	0·617	21·544	21·576	21·671	21·828	22·046	22·324	22·659
	1·234	21·070	21·102	21·199	21·359	21·581	21·864	22·205
	1·851	20·583	20·616	20·715	20·878	21·105	21·393	21·740
	2·465	20·086	20·120	20·221	20·387	20·618	20·912	21·265
1	0	16·222	16·343	16·701	17·280	18·058	19·010	20·110
	0·617	15·962	16·085	16·448	17·036	17·825	18·790	19·902
	1·234	15·696	15·822	16·191	16·788	17·589	18·567	19·692
	1·851	15·426	15·554	15·930	16·537	17·350	18·340	19·480
	2·465	15·153	15·282	15·665	16·282	17·108	18·112	19·266
2	0	15·838	16·051	16·674	17·661	18·952	20·485	22·208
	0·617	15·590	15·807	16·440	17·441	18·748	20·298	22·036
	1·234	15·339	15·559	16·202	17·218	18·541	20·108	21·863
	1·851	15·083	15·307	15·961	16·992	18·333	19·917	21·688
	2·465	14·823	15·052	15·717	16·763	18·122	19·725	21·513
3	0	15·700	16·005	16·886	18·254	20·003	22·036	24·275
	0·617	15·457	15·767	16·661	18·048	19·816	21·868	24·124
	1·234	15·211	15·526	16·434	17·839	19·628	21·698	23·972
	1·851	14·960	15·281	16·203	17·628	19·437	21·528	23·819
	2·465	14·705	15·032	15·970	17·415	19·246	21·356	23·665
4	0	15·630	16·026	17·157	18·883	21·048	23·521	26·208
	0·617	15·390	15·792	16·940	18·687	20·874	23·367	26·071
	1·234	15·145	15·555	16·720	18·490	20·699	23·212	25·933
	1·851	14·897	15·314	16·497	18·289	20·522	23·056	25·794
	2·465	14·645	15·069	16·271	18·088	20·344	22·899	25·656

where a_{k+4} can be determined by the recurrence formula given by equations (30) and (31). The numerical bisection method for root-finding is then used to solve for the non-dimensional modal frequencies Ω_i of the frequency equation (45) for different values of J_0, U, N and η. The results are shown in the next section.

4. RESULTS

The non-dimensional modal frequencies Ω_i in equation (45) obtained by the power series method is solved using the bisection method of root-finding for different values of axial force U, end mass N, beam angular velocity η and total moment of inertia about the hub J_0. The whole calculation is performed using double-precisioin FORTRAN programs.

In this paper, numerical results are presented for $J_0 = 3$ in Tables 1–3 and Figures 2–16. Table 1 gives the calculated values of the non-dimensional first modal

TABLE 3

Non-dimensional third modal frequencies Ω_3 under different end masses N, axial forces U and beam angular velocities η for $J_0 = 3$

		Third mode Ω_3						
N	U	$\eta = 0$	$\eta = 0{\cdot}5$	$\eta = 1{\cdot}0$	$\eta = 1{\cdot}5$	$\eta = 2{\cdot}0$	$\eta = 2{\cdot}5$	$\eta = 3{\cdot}0$
0	0	61·688	61·722	61·824	61·994	62·232	62·535	62·904
	0·617	61·300	61·335	61·437	61·608	61·847	62·152	62·523
	1·234	60·910	60·944	61·048	61·220	61·460	61·767	62·140
	1·851	60·517	60·552	60·656	60·829	61·070	61·379	61·754
	2·465	60·124	60·159	60·263	60·437	60·680	60·991	61·368
1	0	50·887	51·026	51·443	52·130	53·076	54·268	55·690
	0·617	50·614	50·754	51·173	51·864	52·815	54·012	55·441
	1·234	50·340	50·481	50·902	51·596	52·552	53·756	55·191
	1·851	50·064	50·207	50·629	51·327	52·288	53·498	54·940
	2·465	49·789	49·931	50·357	51·058	52·024	53·240	54·689
2	0	50·440	50·687	51·419	52·617	54·249	56·277	58·658
	0·617	50·171	50·419	51·155	52·359	53·999	56·036	58·427
	1·234	49·901	50·150	50·890	52·100	53·748	55·794	58·197
	1·851	49·628	49·879	50·623	51·840	53·496	55·551	57·964
	2·465	49·356	49·608	50·357	51·579	53·244	55·309	57·731
3	0	50·284	50·638	51·683	53·379	55·664	58·470	61·721
	0·617	50·017	50·372	51·422	53·127	55·423	58·241	61·504
	1·234	49·747	50·104	51·160	52·873	55·180	58·010	61·286
	1·851	49·476	49·835	50·897	52·618	54·937	57·778	61·067
	2·465	49·205	49·566	50·634	52·364	54·693	57·547	60·849
4	0	50·205	50·665	52·020	54·201	57·112	60·646	64·698
	0·617	49·938	50·400	51·762	53·954	56·878	60·425	64·487
	1·234	49·669	50·134	51·503	53·705	56·642	60·203	64·283
	1·851	49·399	49·866	51·242	53·455	56·406	59·982	64·076
	2·465	49·128	49·598	50·982	53·206	56·170	59·761	63·868

frequencies Ω_1 under different end masses N, axial forces U and beam angular velocities η. Tables 2 and 3 give the values of the non-dimensional second and third modal frequencies (Ω_2 and Ω_3) respectively under different end masses N, axial forces U and beam angular velocities η. Table 4 gives a comparison of the present numerical results of the modal frequencies for $\eta = 0$ and $J_0 = 10{,}000$ with the results in Ref. [16] and good agreement for the above results was found. The 2-D plots of the non-dimensional modal frequencies Ω_i as functions of end mass N and axial force U under different beam angular velocity η are shown in Figures 2–4. The 2-D plots of the non-dimensional modal frequencies Ω_i as functions of beam angular velocity η under different axial force U and end mass N are shown in Figures 5–10. The 3-D plots of the non-dimensional modal frequencies Ω_i as functions of beam angular velocity η and end mass N for different axial force U are shown in Figures 11–13. The 3-D plots of the non-dimensional modal frequencies Ω_i as functions of beam angular velocity η and axial force U for different end mass N are shown in Figures 14–16.

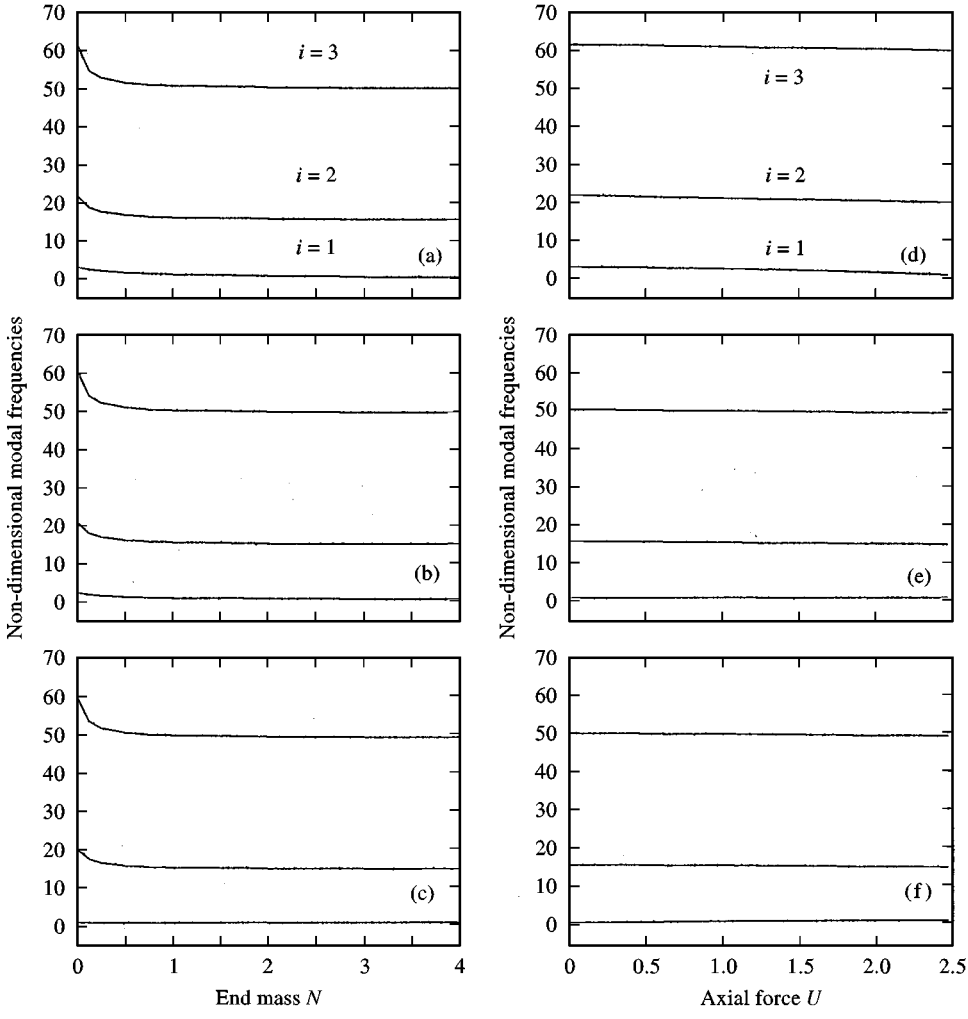

Figure 2. Non-dimensional modal frequencies Ω_i as functions of end mass N and axial force U for beam angular velocity $\eta = 0$. Values of U: (a) 0; (b) 1·234; (c) 2·465. Values of N: (d) 0; (e) 2; (f) 4.

It can be seen from Figure 2 and Figures 11–13 that at $\eta = 0$, an increase in the end mass N causes a decrease in the non-dimensional modal frequencies Ω_i for all the vibration modes and axial force U. The frequency shows a larger decrease rate at lower values of end mass for the second and third modes. However, for $\eta > 0$ (Figures 3, 4 and 11–13), both the second and the third modal frequencies show a decrease at lower values of end mass N, but increase again for larger values of N. The greater the values of η, the larger will be the frequency increase rate for larger values of N. For the first vibration mode, the frequency will always decrease with an increase in N. Figures 5–10 show that an increase in η causes an increase in the frequencies Ω_i of all the vibration modes under different values of end mass N and axial force U.

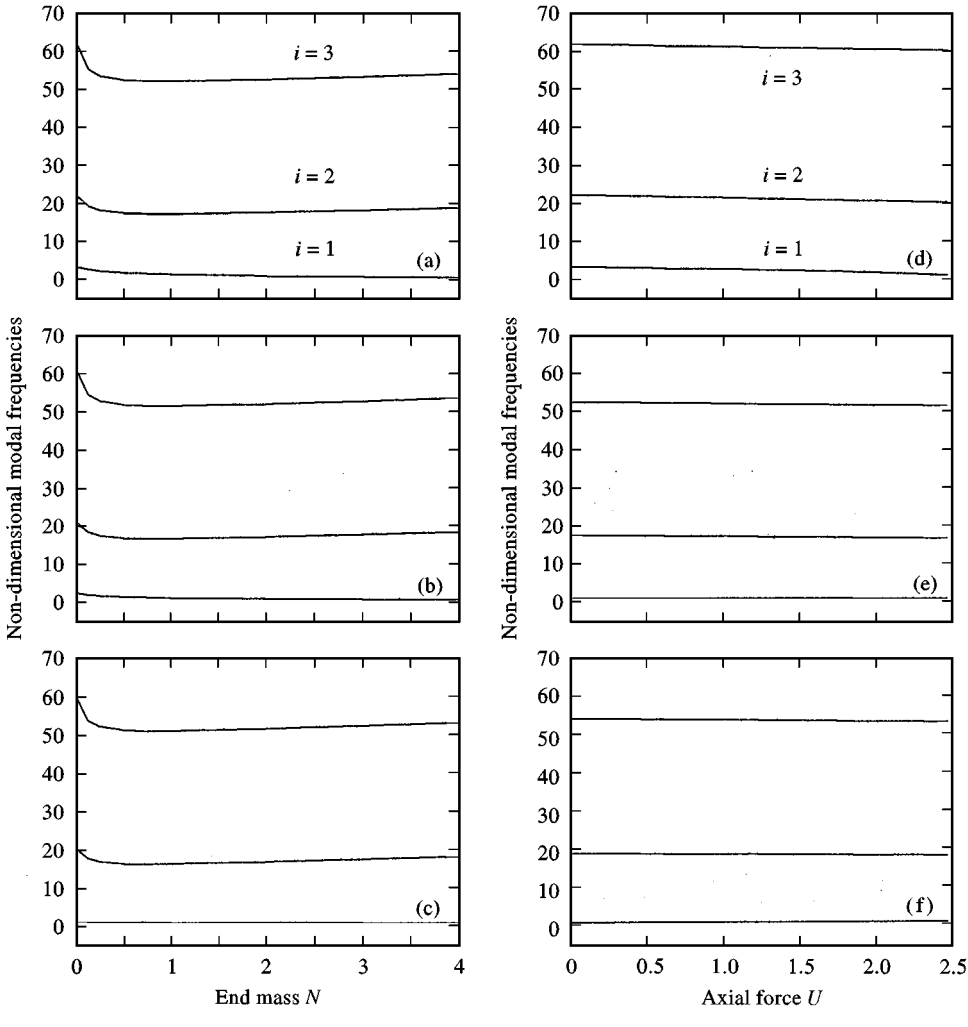

Figure 3. Non-dimensional modal frequencies Ω_i as functions of end mass N and axial force U for beam angular velocity $\eta = 1{\cdot}5$. Values of U: (a) 0; (b) 1·234; (c) 2·465. Values of N: (d) 0; (e) 2; (f) 4.

Figures 2–4 and 14–16 show that an increase in the axial compressive force U causes a decrease in the non-dimensional modal frequencies Ω_i for the second and the third modes of vibration under different values of η and N. In general, the rate of decrease in frequency due to an increase in axial force is more or less constant. For the first vibration mode, an increase in the axial compressive force U causes a decrease in the non-dimensional modal frequency Ω_l for $N = 0$ and 2 under different values of η (Figures 14 and 15). However, for $N = 4$, an increase in the axial compressive force U causes an increase in the non-dimensional modal frequencies Ω_l under different values of η (Figure 16).

5. CONCLUSIONS

In this paper, the equation of motion of a constrained rotating flexible arm is developed using the Euler–Bernoulli beam theory in which the rotary inertia and

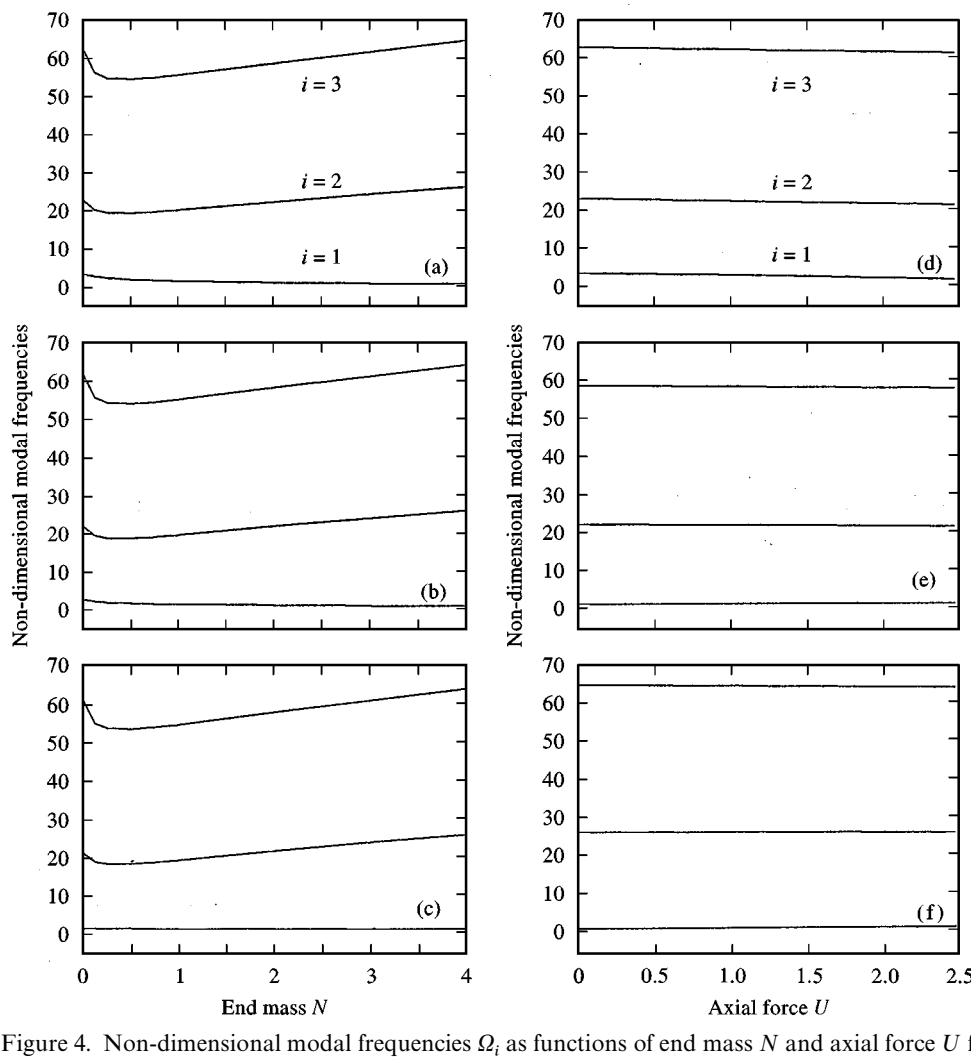

Figure 4. Non-dimensional modal frequencies Ω_i as functions of end mass N and axial force U for beam angular velocity $\eta = 3{\cdot}0$. Values of U: (a) 0; (b) 1·234; (c) 2·465. Values of N: (d) 0; (e) 2; (f) 4.

shear deformation effects are ignored. Hamilton's principle is used to derive the equation of motion and the boundary conditions of the beam. The non-homogeneous boundary condition is transformed into a homogeneous one by defining a new variable. The power series method is used to solve the equation of motion of the rotating beam. A frequency equation is derived giving the relationship between the non-dimensional modal frequency Ω_i and the four non-dimensional parameters, i.e. the axially compressed force U, the end mass N, the angular velocity of the rotating beam η and the total moment of inertia about the hub J_0. Numerical solutions of the frequency equation for $J_0 = 3$ are obtained using double-precision FORTRAN programs. It was found that in general the modal frequency increases with an increase in the beam angular velocity, but decreases as the axial force U is increased except for the first vibration mode with $N = 4$ where the frequencies will increase

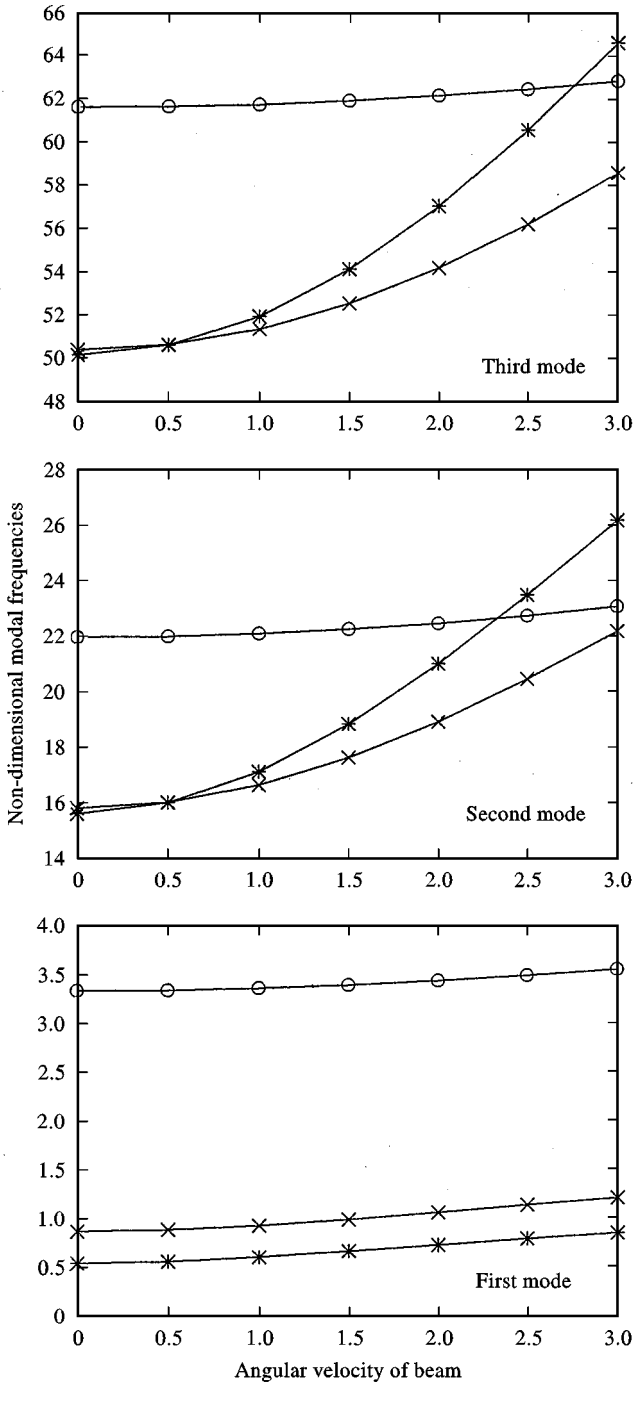

Figure 5. Non-dimensional modal frequencies Ω_i as function of beam angular velocity η for axial force $U = 0$. Values of end mass N: $-\bigcirc- \ N = 0$; $-\times- \ N = 2$; $-*- \ N = 4$.

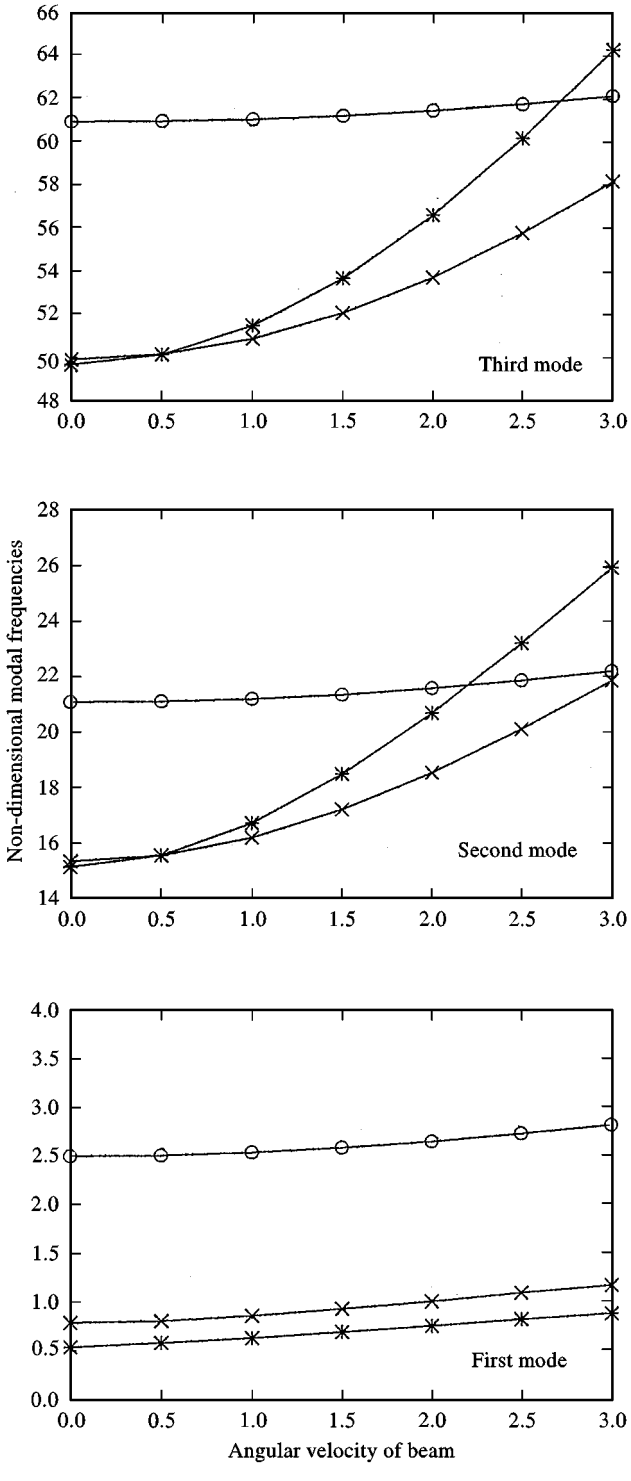

Figure 6. Non-dimensional modal frequencies Ω_i as function of beam angular velocity η for axial force $U = 1{\cdot}234$. Values of end mass N: $-\bigcirc- \; N = 0$; $-\times- \; N = 2$; $-*- \; N = 4$.

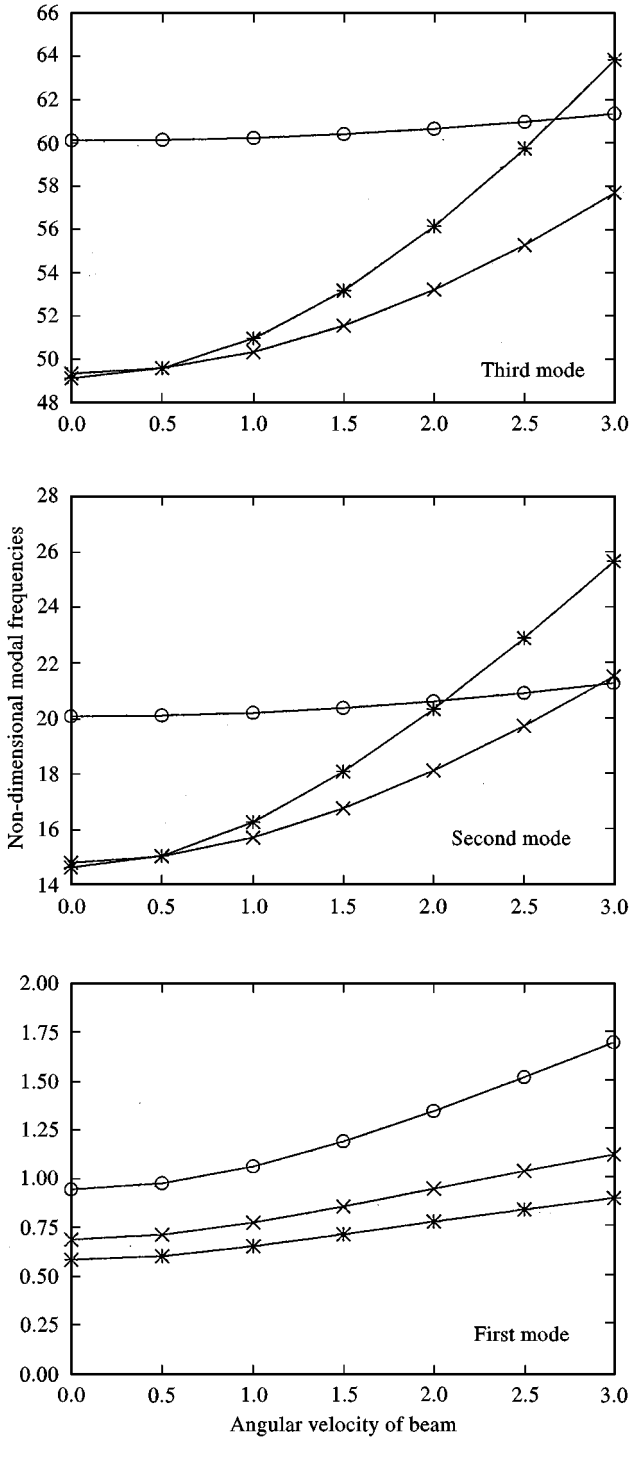

Figure 7. Non-dimensional modal frequencies Ω_i as function of beam angular velocity η for axial force $U = 2{\cdot}465$. Values of end mass N: $-\bigcirc- \; N = 0$; $-\times- \; N = 2$; $-*- \; N = 4$.

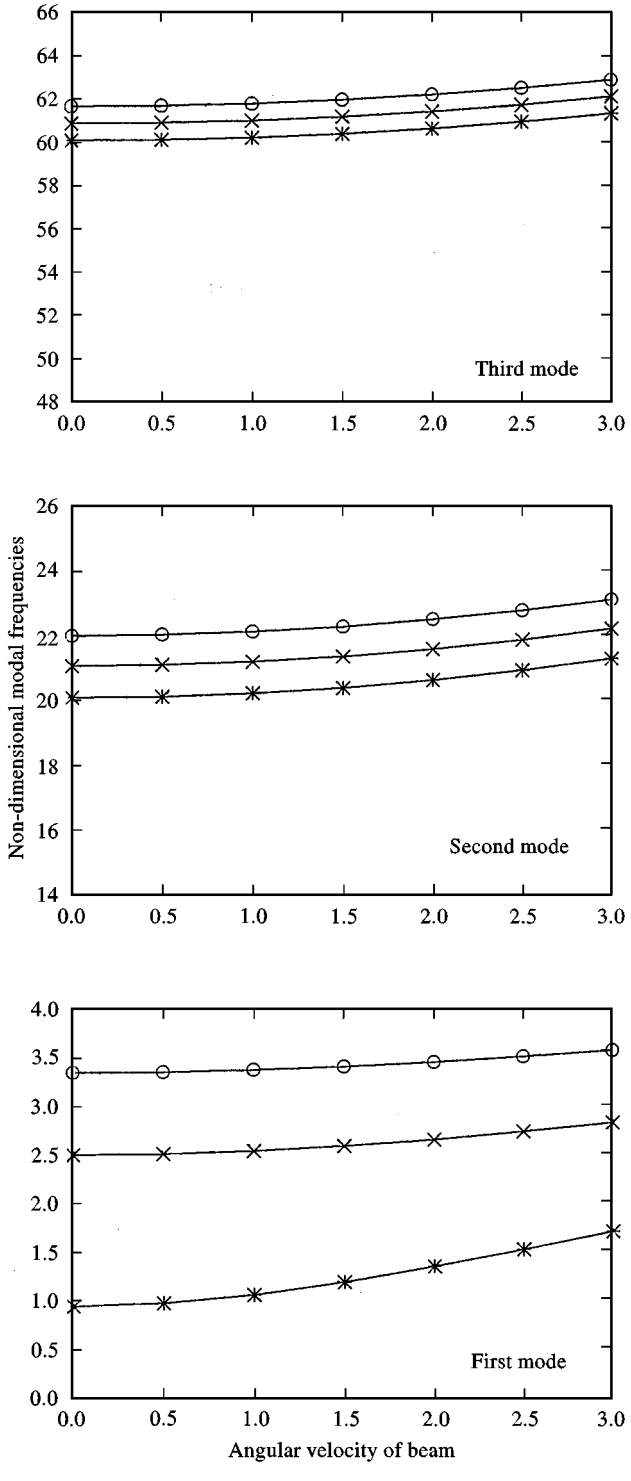

Figure 8. Non-dimensional modal frequencies Ω_i as function of beam angular velocity η for end mass $N = 0$. Values of axial force U: –○– $U = 0$; –×– $U = 1{\cdot}234$; –∗– $U = 2{\cdot}465$.

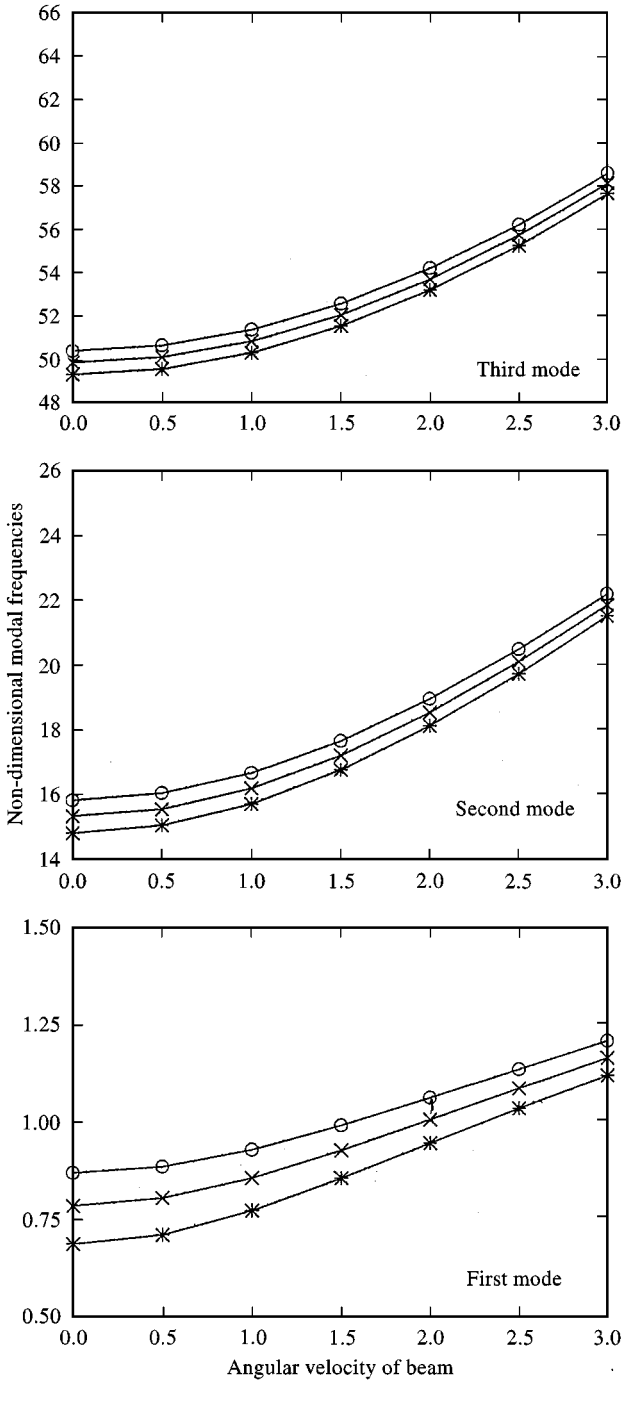

Figure 9. Non-dimensional modal frequencies Ω_i as function of beam angular velocity η for end mass $N = 2$. Values of axial force U: $-\bigcirc- \ U = 0$; $-\times- \ U = 1{\cdot}234$; $-*- \ U = 2{\cdot}465$.

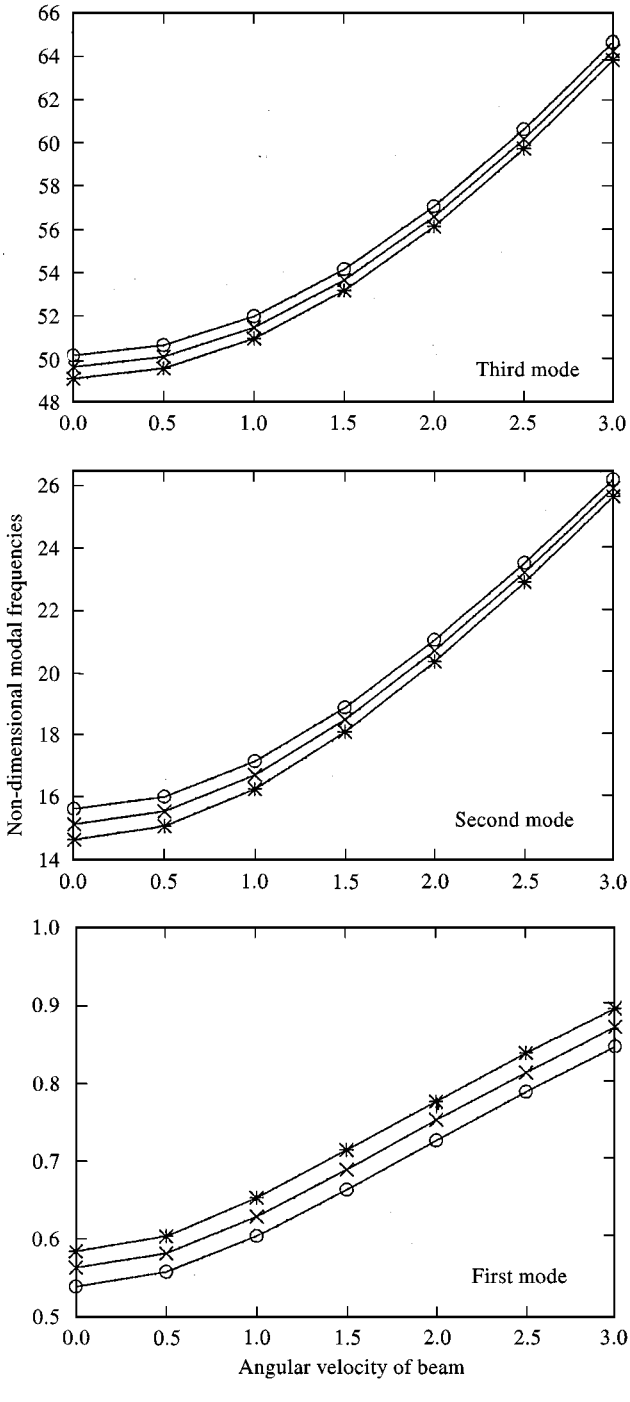

Figure 10. Non-dimensional modal frequencies Ω_i as function of beam angular velocity η for end mass $N = 4$. Values of axial force U: $-\bigcirc- \ U = 0$; $-\times- \ U = 1{\cdot}234$; $-*- \ U = 2{\cdot}465$.

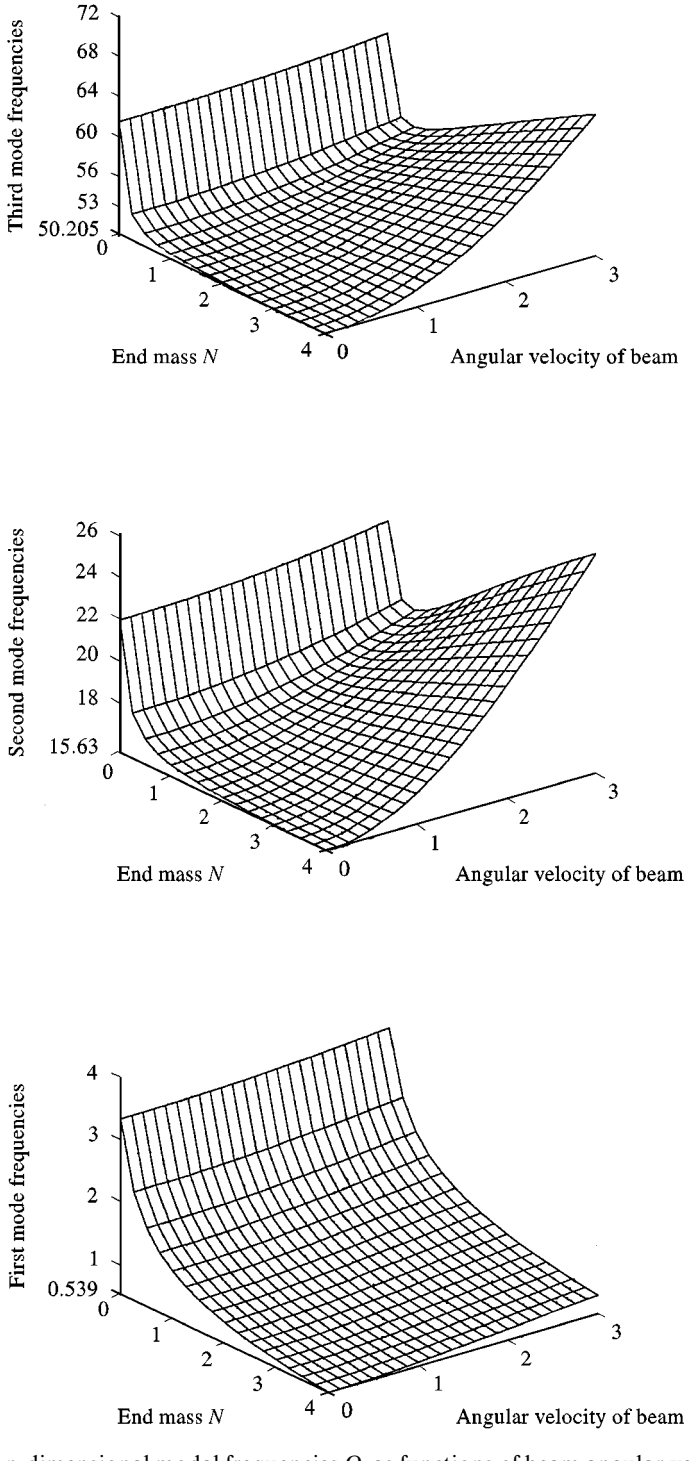

Figure 11. Non-dimensional modal frequencies Ω_i as functions of beam angular velocity η and end mass N for axial force $U = 0$.

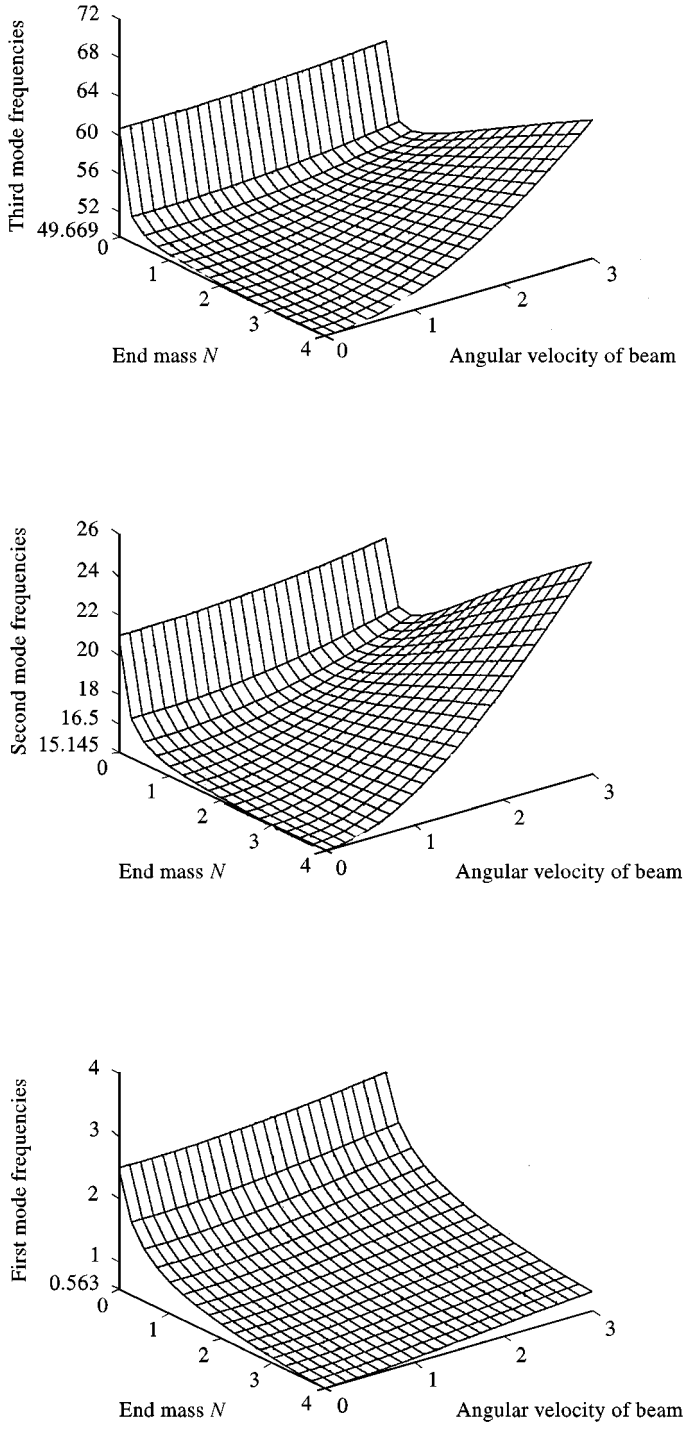

Figure 12. Non-dimensional modal frequencies Ω_i as functions of beam angular velocity η and end mass N for axial force $U = 1{\cdot}234$.

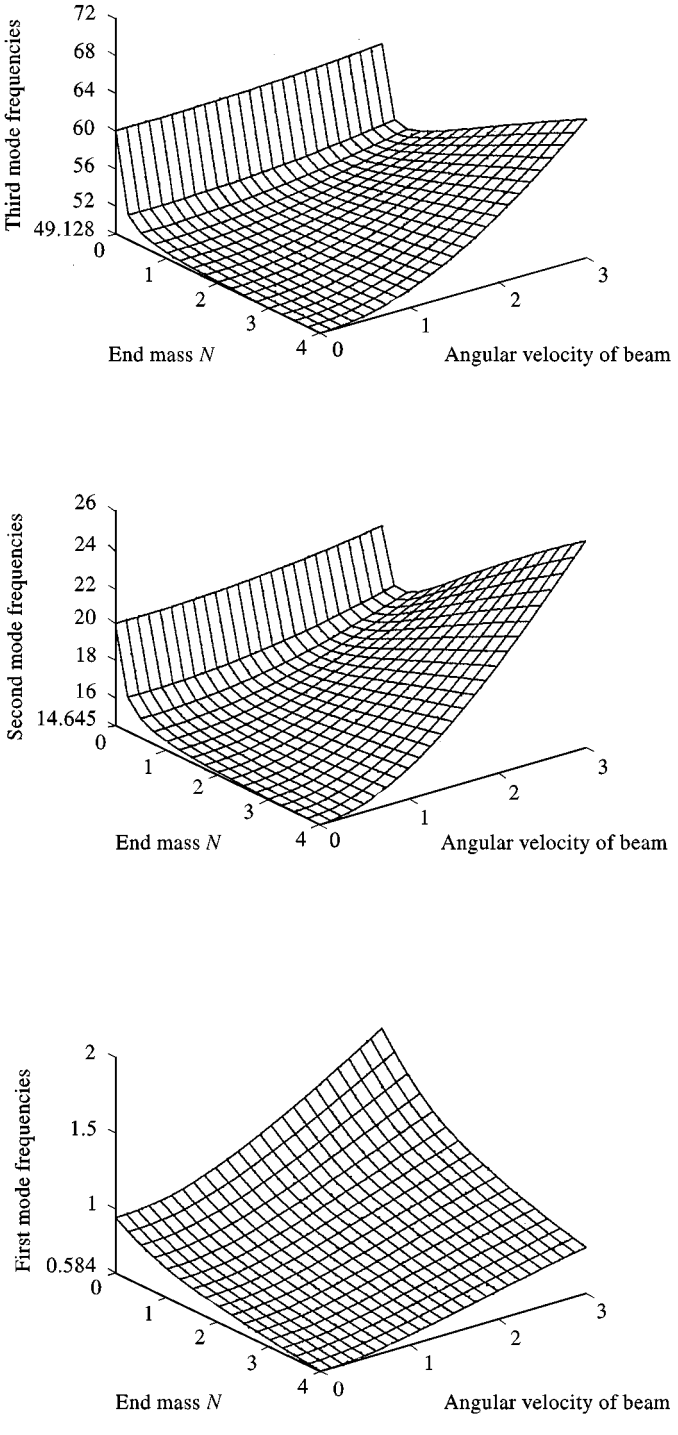

Figure 13. Non-dimensional modal frequencies Ω_i as functions of beam angular velocity η and end mass N for axial force $U = 2{\cdot}465$.

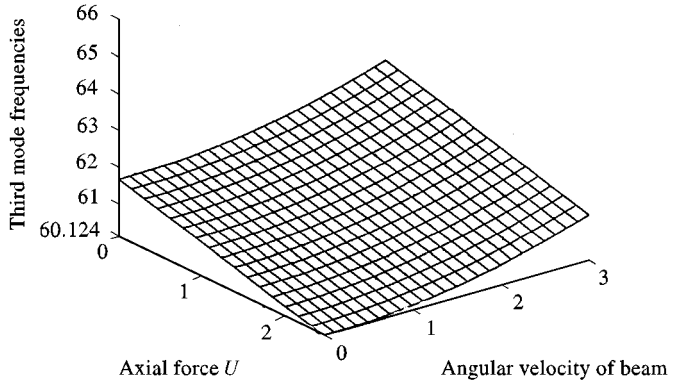

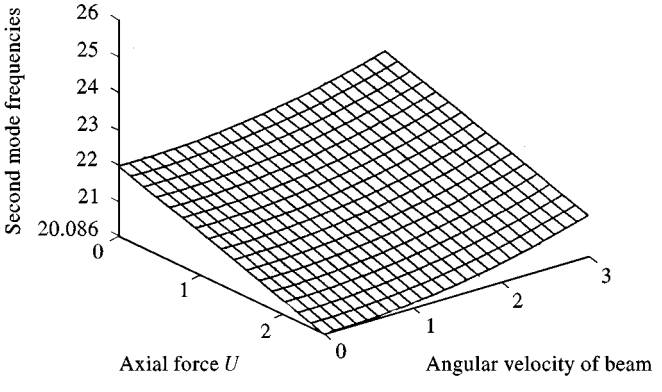

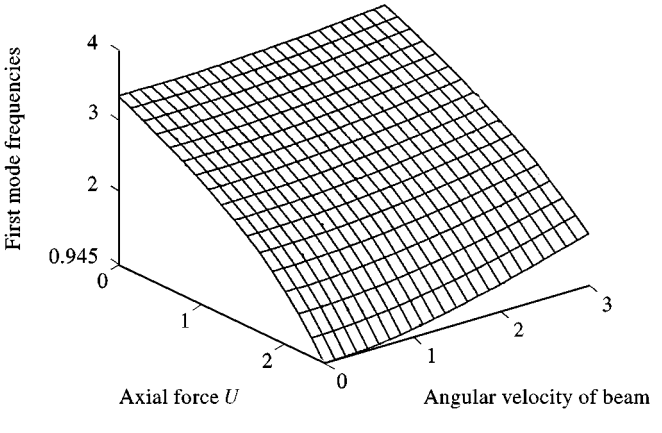

Figure 14. Non-dimensional modal frequencies Ω_i as functions of beam angular velocity η and axial force U for end mass $N = 0$.

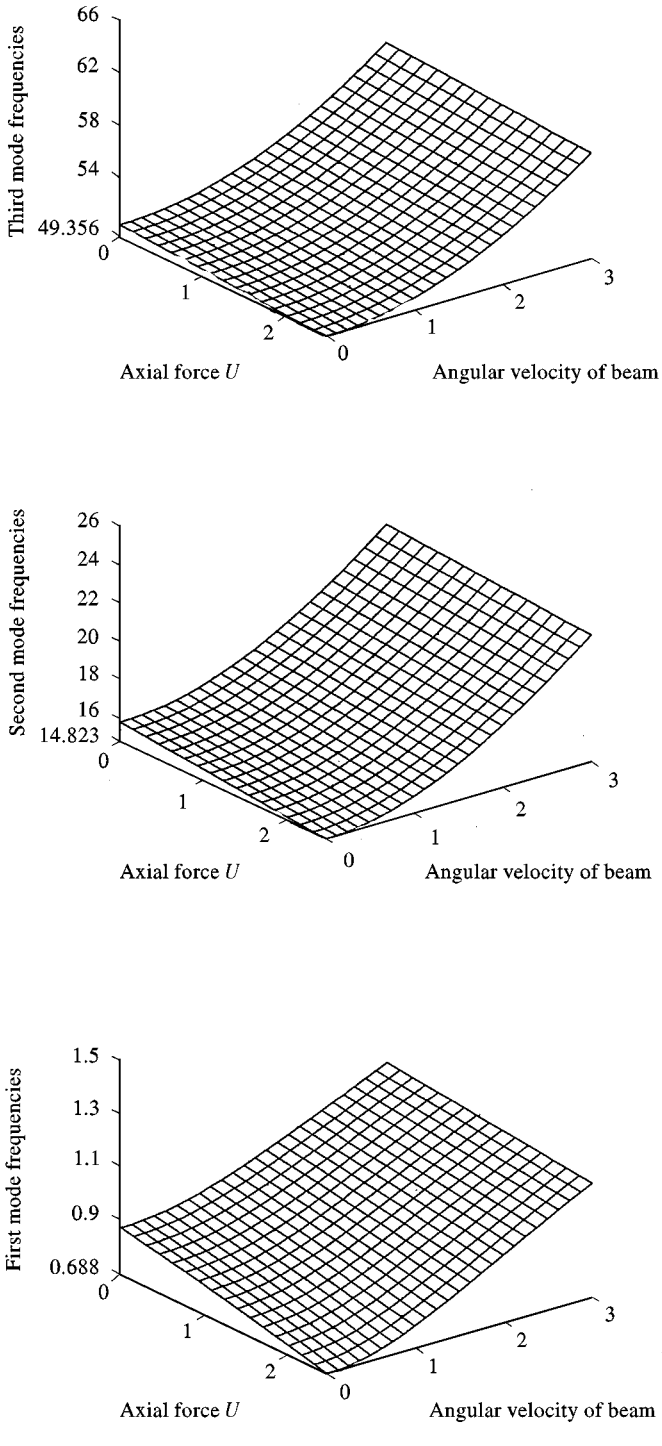

Figure 15. Non-dimensional modal frequencies Ω_i as functions of beam angular velocity η and axial force U for end mass $N = 2$.

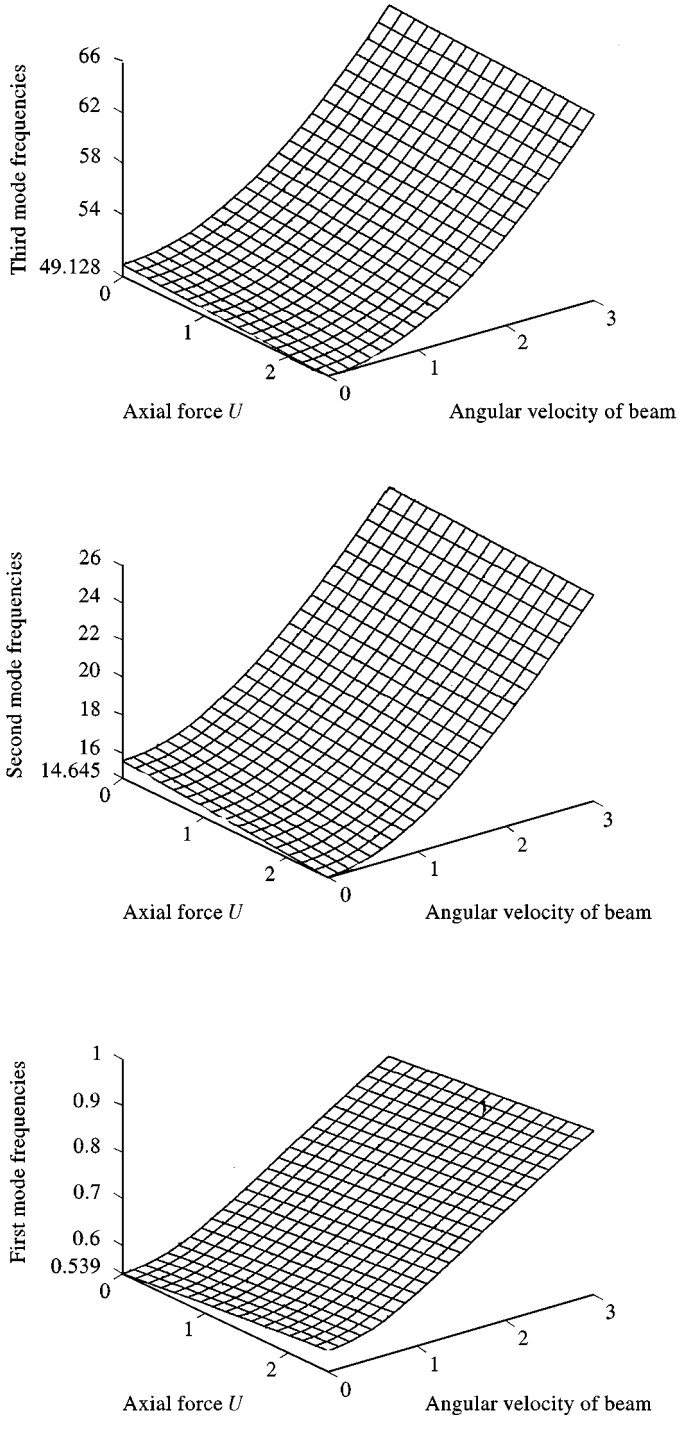

Figure 16. Non-dimensional modal frequencies Ω_i as functions of beam angular velocity η and axial force U for end mass $N = 4$.

TABLE 4
Comparison of present numerical results ($J_0 = 10{,}000$ *and* $\eta = 0$) *with results in reference* [16]

N	U	Ω_1	Reference [16]	Ω_2	Reference [16]	Ω_3	Reference [16]
0	0	3·516	3·516	22·034	22·035	61·697	61·697
	0·617	3·073	3·074	21·575	21·575	61·309	61·310
	1·234	2·534	2·535	21·105	21·105	60·920	60·919
	1·851	1·811	1·811	20·623	20·623	60·527	60·527
	2·465	0·116	0·116	20·131	20·131	60·134	60·133
1	0	1·557	1·557	16·250	16·250	50·896	50·896
	0·617	1·352	1·352	15·991	15·991	50·623	50·623
	1·234	1·107	1·107	15·727	15·727	50·349	50·349
	1·851	0·785	0·707	15·459	15·459	50·074	50·074
	2·465	0·052	0·050	15·187	15·187	49·798	49·798
2	0	1·158	1·158	15·861	15·861	50·447	50·448
	0·617	1·005	1·005	15·615	15·615	50·179	50·179
	1·234	0·823	0·823	15·364	15·364	49·908	49·909
	1·851	0·583	0·583	15·109	15·109	49·636	49·636
	2·465	0·040	0·037	14·851	14·851	49·364	49·364
3	0	0·963	0·963	15·720	15·720	50·291	50·291
	0·617	0·835	0·836	15·478	15·478	50·023	50·023
	1·234	0·684	0·684	15·232	15·232	49·754	49·754
	1·851	0·484	0·485	14·982	14·982	49·483	49·483
	2·465	0·034	0·031	14·729	14·729	49·211	49·212
4	0	0·841	0·842	15·647	15·647	50·211	50·211
	0·617	0·730	0·730	15·407	15·408	49·944	49·944
	1·234	0·597	0·597	15·164	15·164	49·675	49·675
	1·851	0·423	0·423	14·916	14·917	49·404	49·405
	2·465	0·031	0·027	14·666	14·666	49·134	49·134

with increase in axial force. For stationary constrained beams ($\eta = 0$), the frequency shows a decrease with an increase in end mass N. For rotating constrained beams ($\eta > 0$) at the second and third modes, the frequency shows a decrease at lower values of N but an increase for larger values of N, and its increase rate is higher for larger values of η. For the first mode of vibration, the frequency will always decrease with an increase in N. These results can be applied to other practical engineering problems that involve rotation of constrained flexible beams.

ACKNOWLEDGMENTS

This research work was supported by The Hong Kong Polytechnic University Research Grant Committee under project account code 0351.101.A3.430(G-S145). The authors wish to thank the reviewers for their useful comments.

REFERENCES

1. A. Bokaian 1988 *Journal of Sound and Vibration* **126**, 49–65. Natural frequencies of beams under compressive axial loads.
2. N. G. Stephen 1989 *Journal of Sound and Vibration* **131**, 345–350. Beam vibration under compressive axial load — upper and lower bound approximation.
3. A. Bokaian 1990 *Journal of Sound and Vibration* **142**, 481–498. Natural frequencies of beams under tensile axial loads.
4. H. Matsunaga 1996 *Journal of Sound and Vibration* **191**, 917–933. Free vibration and stability of thin elastic beams subjected to axial force.
5. X. Q. Liu and R.C. Ertekin 1996 *Journal of Sound and Vibration* **190**, 273–282. Vibration of a free-free beam under tensile axial loads.
6. M. W. D. White and G. R. Heppler 1995 *ASME Journal of Applied Mechanics* **62**, 193–199. Vibration modes and frequencies of Timoshenko beams with attached rigid bodies.
7. M. W. D. White and G. R. Heppler 1996 *ASME Journal of Vibration and Acoustics* **118**, 606–613. Vibration of a rotating Timoshenko beam.
8. A. S. Yigit 1992 *ASME Advances in Robotics* DSC-**42**, 229–232, A robust controller for a two-link rigid flexible manipulator.
9. A. S. Yigit, R. A. Scott and A. Galip Ulsoy 1988 *Journal of Sound and Vibration* **121**, 201–210. Flexural motion of a radially rotating beam attached to a rigid body.
10. S. Choura and S. Jayasuriya, 1991 *ASME Journal of Dynamic Systems, Measurement, and Control* **113**, 26–33. On the modeling, and open-loop control of a rotating thin flexible beam.
11. C. M. Oakley and R. H. Cannon, Jr. 1989. *Proceedings of the American Control Conference*, 1381–1388. End-point control of a two-link manipulator with a very flexible forearm: issues and experiments.
12. H. Du, M. K. Lim and K. M. Liew 1994 *Journal of Sound and Vibration* **175**, 505–523. A power series solution for vibration of a rotating Timoshenko beam.
13. J. C. Simo and L. Vu-Quoc 1987 *Journal of Sound and Vibration* **119**, 487–508. The role of non-linear theories in transient dynamic analysis of flexible structures.
14. B. Fallahi, S. H. Y. Lai and R. Gupta 1994 *ASME Journal of Vibration and Acoustics* **116**, 93–99. Full beam formulation of a rotating beam–mass system.
15. K. D. Murphy and C. L. Lee 1998 *Journal of Sound and Vibration* **211**, 179–194. The 1 : 1 internally resonant response of a cantilever beam attached to a rotating body.
16. E. H. K. Fung and Z. X. Shi 1997 *Journal of Sound and Vibration* **204**, 259–269. Vibration frequencies of a constrained flexible arm carrying an end mass.
17. W. H. Press, B. P. Flannery, S. A. Teukolsky and W. T. Vetterling 1986. *Numerical Recipes*. Cambridge: Cambridge University Press.

APPENDIX: NOMENCLATURE

EI	flexural rigidity of flexible beam
f	function defined in equation (9)
f_n	reaction force along **n**
g	function defined in equation (9)
J	moment of inertia of the hub
J_t	total moment of inertia about the hub
J_0	non-dimensional form of J_t
L	length of flexible beam
m	end mass
N	non-dimensional end mass
η	non-dimensional angular velocity of flexible beam

$P((r, t)$	centrifugal force arising from centrifugal effect
q_i	generalized co-ordinate
Q	axial force along **i**
r	position of a point on flexible beam
t	time
T	total kinetic energy of flexible arm
U	non-dimensional axial force
τ	torque developed by motor
τ_1	load torque exerted on motor
μ_i	torque defined in equation (20b)
μ_0	non-dimensional form of μ_i
v	variable defined in equation (12)
V	total potential energy of flexible arm
w	transverse displacement of flexible beam
w_E	transverse displacement at tip of flexible beam
X_p, Y_p	co-ordinates of end point of flexible beam
Y_i	mode shape function defined in equation (12)
θ	hub angle of flexible beam
$\dot{\theta}$	angular velocity of flexible beam
Φ	constrained curve function
λ	Lagrange multiplier associated with the constrained curve
ρ	mass per unit length of flexible beam
δW	virtual work
ω_i	modal frequency of flexible beam
Ω_i	non-dimensional modal frequency of flexible beam
ξ	non-dimensional spatial co-ordinate
P	position vector of end point of flexible beam
r	position vector of a point on flexible beam
(**i**, **j**)	a pair of orthogonal unit vectors for flexible beam
n	normal direction of constrained curve